Available online at www.sciencedirect.com
SCIENCE DIRECT®
Biochemical and Biophysical Research Communications 324 (2004) 281–287
BBRC
www.elsevier.com/locate/ybbrc

Topogenesis of NHE1: direct insertion of the membrane loop and sequestration of cryptic glycosylation and processing sites just after TM9

Yoko Sato[a,b], Naoko Ariyoshi[b], Katsuyoshi Mihara[b], Masao Sakaguchi[a,b,c,*]

[a] *Graduate School of Life Science, University of Hyogo, Ako, Hyogo 678-1297, Japan*
[b] *Graduate School of Medical Science, Kyushu University, Fukuoka 812-8582, Japan*
[c] *CREST of Japan Science and Technology Agency, Ako, Hyogo 678-1297, Japan*

Received 1 September 2004
Available online 25 September 2004

Abstract

Multispanning membrane proteins are synthesized by membrane-bound ribosomes and integrated into the endoplasmic reticulum membrane cotranslationally. To uncover the topogenic process of membrane loop, of which both ends are in the same side of the membrane, we examined topogenesis of a relatively hydrophobic lumenal loop segment (H10 segment) between TM9 and TM10 of human Na^+/H^+ exchanger isoform 1 using an in vitro expression system. The H10 segment was translocated through the membrane. Any potential sites created within the H10 segment were not glycosylated. Just after TM9, there are potential glycosylation and signal peptidase processing sites. When the reporter domain of prolactin was fused at the position preceding the H10 segment, these sites were modified by the enzymes, while they were not modified in the original molecule. Thus, we concluded that the H10 segment was translocated through the membrane and directly inserted into the membrane and that its membrane insertion caused sequestration of the preceding processing and glycosylation sites from the lumenal modifying enzymes. This topogenic process shows clear contrast to that of pore loops of K^+ channels, which are once exposed in the lumen and accessible to glycosylation enzyme.

Keywords: NHE; Topogenesis; Transmembrane; Topology; Processing; Glycosylation

Almost all of the integral membrane proteins on membrane organelles of the exocytic and endocytic pathway are synthesized on membrane-bound ribosomes and cotranslationally integrated into the endoplasmic reticulum (ER) membrane, where they acquire their final topology [1]. Initially, a signal sequence on the nascent polypeptide chain emerging from the ribosome is recognized by the signal recognition particle (SRP) [2]. The ribosome–SRP–nascent chain complex is targeted to the ER, where there is an SRP receptor and protein translocation channel, the so-called "translocon" [3]. By the receptor, the signal sequence is released from the SRP and is transferred to the translocon. The signal sequence is then recognized by the translocon and penetrates it. At this stage, either the preceding N-terminal or the following C-terminal segment of the signal sequence is translocated through the translocon pore [4]. The signal peptide and type II signal anchor sequence (SA-II sequence) mediate the translocation of the following C-terminal side, while the type I signal anchor sequence (SA-I sequence) translocates the preceding N-terminal side [5,6]. Once targeted to the ER membrane, the ribosome remains on the translocon until translation is terminated, even while it is synthesizing the cytoplasmic sequence.

* Corresponding author. Fax: +81 791 58 0132.
E-mail address: sakag@sci.u-hyogo.ac.jp (M. Sakaguchi).

0006-291X/$ - see front matter © 2004 Elsevier Inc. All rights reserved.
doi:10.1016/j.bbrc.2004.09.054

Three experimentally defined topogenic mechanisms have been proposed for the membrane integration of polypeptide segments from membrane-bound ribosomes. First, hydrophobic segments are inserted into the translocon by sequential action of their start-transfer and stop-transfer functions. This mechanism is called autonomous membrane insertion [7]. For the start-transfer and stop-transfer functions, sufficient hydrophobicity is essential. Second, when the SA-I sequence acts in the multispanning membrane protein molecule, the polypeptide segment, which possesses no topogenic function and cannot be inserted into the membrane by itself, can acquire transmembrane disposition [8,9]. Such a non-hydrophobic transmembrane (TM) segment would not be fixed in the membrane plane and can be expected to move up and down within the membrane. This mechanism is called heteronomous positioning of the TM segment [7]. Third, some hydrophilic segments are inserted into the membrane domain via polar interactions among TM segments, but not via hydrophobic interactions. This mechanism has been elucidated in various transport proteins; e.g., the membrane insertion of the R10 segment between TM9 and TM10 of the band 3 molecule [10] and the voltage sensing segments (S3 and S4 segments) of KAT1 (*Arabidopsis thaliana*, voltage dependent K^+-channel) [11,12].

Despite the knowledge of topogenic modes of TM segments, membrane insertion of membrane embedded loop segment has not been extensively analyzed. When is relatively hydrophobic loop segment inserted into the membrane? So far, we have examined the topogenesis of the pore loops between two TM segments of K^+ channels, which are typical membrane loops, and demonstrated that the loop is once exposed in the ER lumen before the channel molecule achieves the final membrane topology, despite high hydrophobicity, and a high prediction score for their being transmembrane [13]. The major objective of this study was to address the topogenic process of other membrane-embedded loop segments in multispanning membrane proteins. For the purpose, we selected a hydrophobic loop segment of human Na^+/H^+ exchanger isoform 1 (NHE1) in this study. From comprehensive cysteine scanning experiments with the NHE1 molecule, Wakabayashi et al. [14] proposed a revised model of membrane topology (Fig. 1A); it has 12 TM segments and the hydrophobic loop segment (called H10 in this paper) between TM9 and TM10. The H10 segment was initially predicted to be a TM segment based on hydropathy prediction [15].

We examined the membrane topogenesis of H10 segment of NHE1 molecule using systematically designed model constructs and a cell-free expression system including rough ER membrane and demonstrated that the H10 segment was translocated through the membrane but was not exposed to the lumenal space. We also uncover an unexpected glycosylation and processing sites just after the TM9 segment, which are inaccessible to the effective enzymes during integration of the H10 segment. In the absence of the H10 segment, these modification sites were actually accessible to the enzymes. These data proposed the novel mode of the integration process in the membrane-embedded loop segment. This mode is different from those of the pore loops of the K^+ channels.

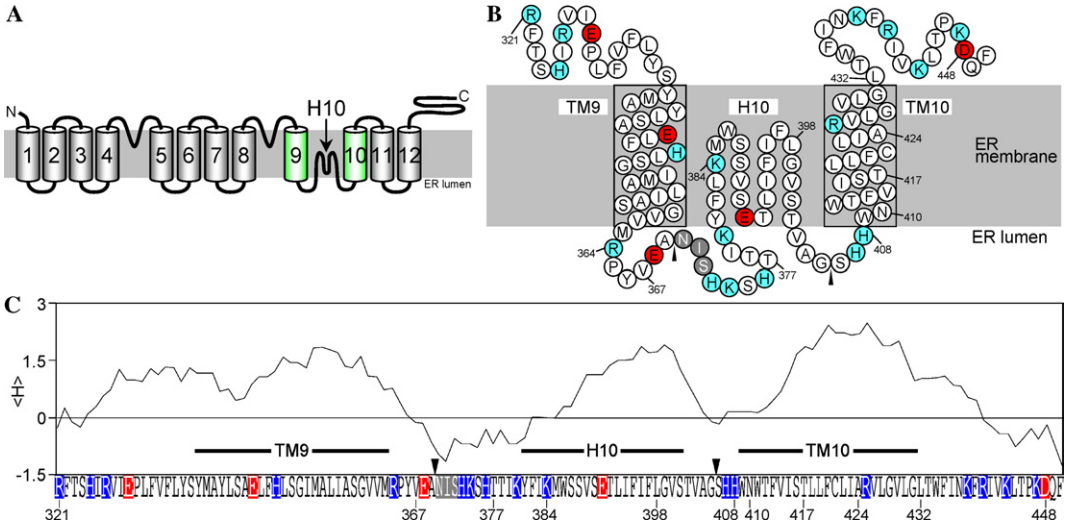

Fig. 1. Membrane topology of NHE1. (A,B) Topology model of human NHE1. Here, the hydrophobic region between TM9 and TM10 is termed the H10 segment. Positively charged residues (blue), negatively charged residues (red), and N-glycosylation acceptor sequence (gray) are indicated. Numbers indicate amino acid residues at which the constructs start or are fused to reporter domain. (C) Hydrophobic profile of TM9–TM10. The plot was generated by the method of Kyte and Doolittle [29]. Potential processing sites are indicated by arrowheads.

Materials and methods

Materials. Enzymes for DNA manipulation and in vitro transcription (Takara), proteinase K (ProK; Merck), and endoglycosidase H (EndoH; New England Biolabs) were obtained from the sources indicated. Preparation of rough microsomal membranes (RM) [16] and rabbit reticulocyte lysate [17] was performed as previously described. To remove endogenous RNA, RM was treated with EDTA and *Staphylococcus aureus* nuclease as described. The plasmid DNA was prepared using Wizard plus mini-preps (Promega) from 2 ml overnight cultures of *Escherichia coli*.

Construction of expression plasmids. cDNA coding for human NHE1 was amplified by PCR using cDNA reverse-transcribed from liver total RNA and the following primers; 5′-ATGCAAGCTTCCACCATGGCTCTGCGGTCT-3′ (the *Hin*dIII sites for cloning, the created Kozak sequence, and the initiation codon of NHE1 are underlined) and 5′-TACGTCTAGAGTTGAGCTTGTCCTTCCAGTG-3′ (the *Xba*I site is underlined). The obtained DNA fragments were digested with *Hin*dIII and *Xba*I, and subcloned into pRcCMV (*Hin*dIII/*Xba*I). Site-directed mutagenesis was performed using the PCR-directed overlap–extension method [18]. In the fusion constructs, the DNA fragments were joined either by restriction enzyme sites, whose six bases correspond to the two codons, or by the overlap–extension procedure. Each DNA fragment (*Nde*I/*Xho*I) encoding various segments of human NHE1, which are initiated from R^{321}, was amplified and ligated with the DNA fragment (*Xho*I/*Xba*I) coding for the reporter domain of prolactin (PL) with/without the glycosylation site (T90N) [9] on pCITE-2a (Novagen) (*Nde*I/*Xba*I) [19]. For the glycosylation-loop (g-loop) insertion, the DNA fragment containing N-glycosylation sites derived from human band 3 (Q^{629}–W^{662}, *Eco*RI/*Eco*RI) [9] was inserted between W^{409} and N^{410} of NHE1. The sequences of oligonucleotides used and details for construction are available upon request from the author.

In vitro transcription, translation, EndoH, and ProK treatment. Plasmids were linearized using *Sca*I and then transcribed using T7 RNA polymerase. The obtained mRNAs were translated in the reticulocyte lysate cell-free system as previously described [5]. The translation reaction mixture contained 100 mM KCl, 1.5 mM $Mg(OAc)_2$, 32% reticulocyte lysate, and 15.5 kBq/μl EXPRESS protein-labeling mix (Perkin–Elmer). Aliquots (10 μl) of translation mixture were treated with EndoH at 37 °C for 60 min under denaturing conditions. Other aliquots were treated with 400 μg/ml ProK on ice for 40 min. After ProK treatment, the reaction was terminated with 10% trichloroacetic acid and the protein precipitates were analyzed by SDS–PAGE and subsequent image analysis.

Results

Topogenic properties of H10 and TM10 segments

In this study, TM segments of human NHE1 were termed according to the nomenclature of Wakabayashi et al. [14]. The hydrophobic segment between TM9 and TM10 was called the H10 segment (Fig. 1). The H10 segment was predicted to be a TM segment based only on the hydrophobicity analysis [15]. To examine the topogenic process of the H10 segment, we evaluated the topogenic functions of the polypeptide segments around H10 and TM10. A reporter domain of PL with an N-glycosylation site (gPL) was fused at various positions from TM9 to TM10 (Fig. 2A). Modification of the N-glycosylation site would be a decisive indication of the membrane topology. The constructs were initiated from the TM9 segment but not from the N-terminus, because the full-length protein possesses so many hydrophobic segments that such a full-length construct causes a very diffuse band on the SDS–PAGE. The topogenic function of the TM9 segment is strong SA-II, so that local topogenic functions (e.g., start- and stop-transfer functions) around the TM9, H10, and TM10 segments should not be affected by the absence of the former TM segments.

The constructed model proteins were expressed in the reticulocyte lysate cell-free system. When translated in the absence of RM, the synthesized molecules gave single major bands with the expected molecular mass (Fig. 2A, lanes 1, 5, 9, 13, 17, 21, and 25). In the presence of RM, the V^{367}-construct gave an additional larger product (a black dot in lane 2), which was shifted down by EndoH treatment (lane 3), indicating that it was core glycosylated and that the reporter domain of prolactin was translocated into the ER lumen. When the translation mixtures were treated with ProK, both of the products observed in lane 2 were completely resistant to ProK (white dots in lane 4). Because the external segment of the molecule is sensitive to ProK, it is clear that a gPL domain of the V^{367}-construct was translocated through the ER membrane and became resistant.

Significant amounts of glycosylated and ProK resistant bands were observed with other fusion constructs up to the H^{408}-construct, although constructs gave heterogeneous bands (Fig. 2A, lanes 6–8, 10–12, 14–16, and 18–20, details of these bands are described in the next section). The relative amounts of the glycosylated form and ProK resistant form decreased as the fusion sites shifted to the latter positions (A^{424} and L^{432} in lanes 22, 24, 26, and 28). These findings indicated that the PL-reporter domains that had been fused up to the H^{408}-construct were fully translocated through the ER membrane, glycosylated, and protected by the ER membrane. The translocation of A^{424}-construct was partially stopped by the former part of TM10 (lanes 22–24). Thus, we concluded that the H10 segment did not have a stop-transfer function and that the translocation initiated by the TM9 segment was stopped only by the TM10 segment.

To confirm the orientation of the H10 segment, the g-loop from human band 3 was inserted between the H10 and TM10 segments (Fig. 2B). This loop possesses little inhibitory effect on the polypeptide chain translocation and thus has often been used for probing membrane topology of multispanning membrane proteins; e.g., band 3, K^+-channel, and various ion transporters [10,12,20,21]. The construct with the g-loop was efficiently glycosylated (a black dot in lane 4), whereas glycosylation was not observed with the original construct (lane 1). After ProK treatment,

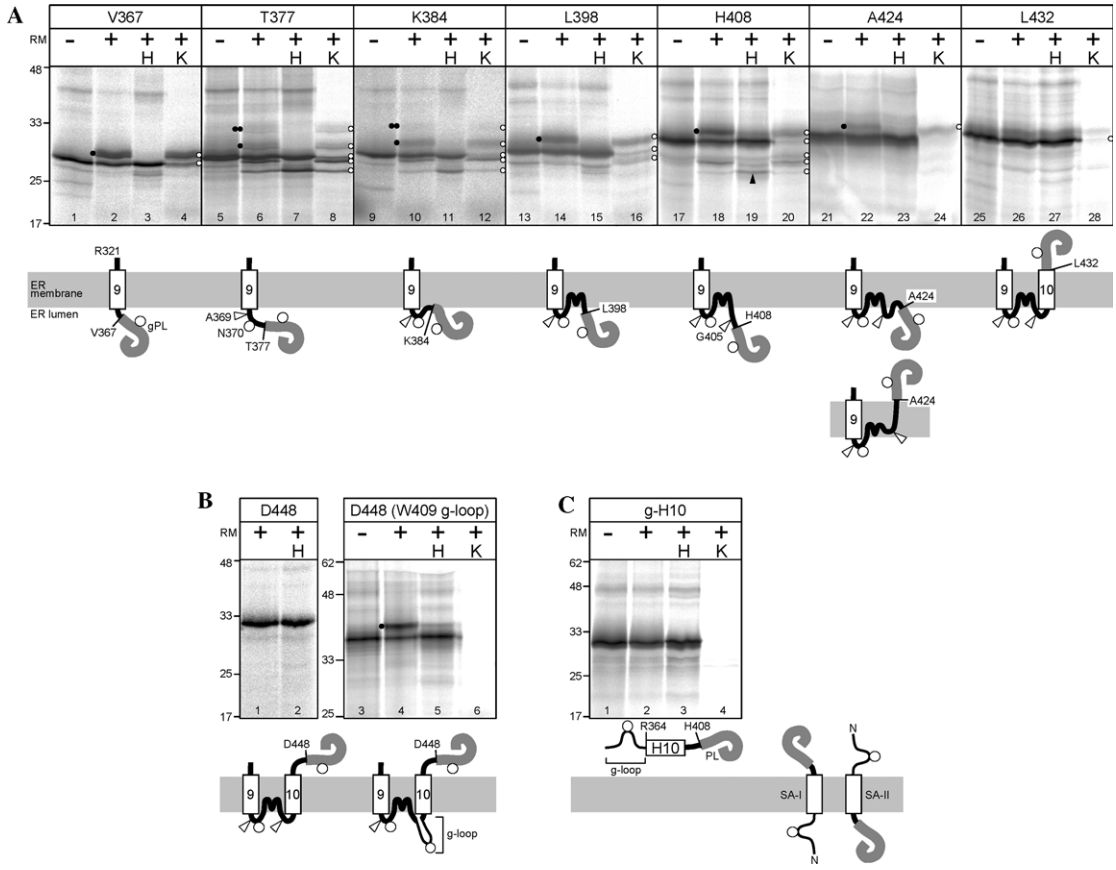

Fig. 2. H10 possesses neither stop nor signal functions. (A) Amino acid sequences, starting at TM9 (R^{321}), were fused to the gPL reporter domain at various sites. The fusion proteins were expressed in vitro in the absence (−) or presence (+) of RM. The aliquots were treated with EndoH (H) or ProK (K). The proteins were subjected to SDS–PAGE (13%) followed by image analysis. The glycosylated and ProK resistant bands are indicated by black and white dots, respectively. A black arrowhead points out PL-reporter domain processed between G^{405} and S^{406} (see text). Topologies deduced from the results are illustrated. The glycosylation and processing sites are shown as circles and white arrowheads, respectively. (B) A 42-residue loop segment containing a glycosylation site was inserted next to W^{409}. (C) Assessment of signal-anchor function with the H10 segment. The H10 segment (R^{364}–H^{408}) was inserted between the N-terminal g-loop and the following PL domain. The PL domain used here does not have a glycosylation site. Membrane topologies expected by the SA-I and SA-II functions are illustrated. The model protein was expressed in vitro and subjected to EndoH and ProK treatment.

there were no resistant bands (lane 6), indicating that the following reporter domain was on the cytoplasmic side. These results are a clear indication that the loop between H10 and TM10 was exposed to the ER lumenal side.

Topogenic functions of the H10 segment were also examined using the constructs shown in Fig. 2C. Translocations of the N- and C-terminal side of the H10 segment can be monitored by N-terminal glycosylation (circle) and C-terminal protease resistance, respectively [9]. The PL domain used here does not have a glycosylation site. The H10 model protein gave neither a glycosylated nor a ProK-resistant fragment (lanes 2 and 4), indicating that the H10 segment possesses no signal-anchor functions. Taken together, the H10 segment does not possess any signal-anchor functions, and TM10 alone was sufficient to stop the translocation that was initiated by TM9.

Potential glycosylation and processing sites between TM9 and TM10

In Fig. 2A, heterogeneous bands, which were one band larger than the mono-glycosylated form and several bands smaller than the unglycosylated form (black and white dots in lanes 6, 8, 10, 12, 18, and 20), were observed when the T^{377}-, K^{384}-, and H^{408}-constructs were translated in the presence of RM. All of the bands were resistant to ProK (e.g., compare lanes 6 and 8) and many bands were shifted by EndoH treatment to generate two major bands (compare lanes 6 and 7), indicating that unexpected glycosylation caused the heterogeneity. The clear two bands after the EndoH treatment strongly suggested that unexpected processing also occurred within the lumenal side.

To address the possibility of glycosylation just after the TM9, we destroyed the potential site

(N^{370}–I^{371}–S^{372}) by point mutation, S372A, using the T^{377}-construct (Fig. 3A). When translated in the presence of RM, it gave only a mono-glycosylated band, although the heterogeneous bands within the smaller forms were still observed (lane 6), indicating that the larger band was due to glycosylation at N^{370} in addition to the glycosylation in the reporter domain. The di-glycosylation efficiency decreased as the fusion site was shifted into the latter position; the K^{384}-construct also gave a small but significant di-glycosylated band (Fig. 2A, lane 10), while di-glycosylation was not observed with the L^{398}-, H^{408}-, A^{424}-, and L^{432}-constructs (lanes 14, 18, 22, and 26). The site was sequestrated from the enzyme due to the H10 segment.

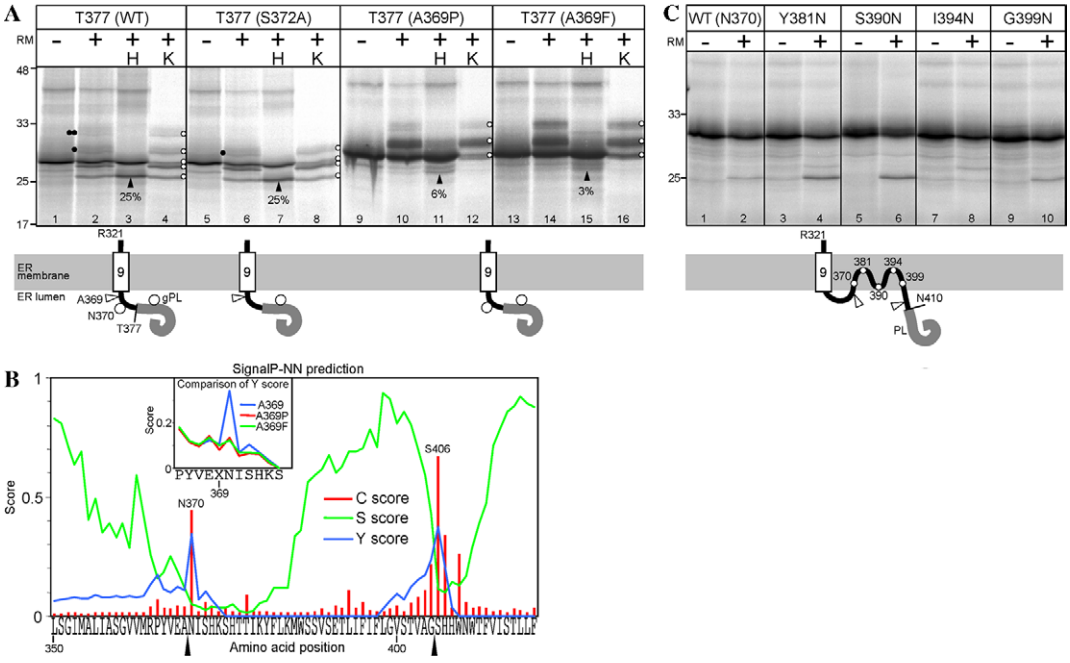

Fig. 3. Assessment of potential glycosylation and processing sites. (A) Potential sites for glycosylation and processing were disrupted by point mutations. The constructs were expressed in vitro and analyzed as described in Fig. 2. Black arrowheads indicate processed from. The processed form efficiencies were calculated using the equation (processed form) × 100/[(non-processed form) + (processed form)]. (B) A signal peptide prediction by SignalP-NN for H10. The values of the C-score (output from cleavage site networks), S-score (output from signal peptide networks), and Y-score (combined cleavage site score) are shown for each position in the sequence. (Inset) Comparison of Y-score derived from with/without mutation. (C) Glycosylation sites were created at various positions in the H10 sequence by point mutations and then expressed in vitro. The PL domain used here does not have a glycosylation site.

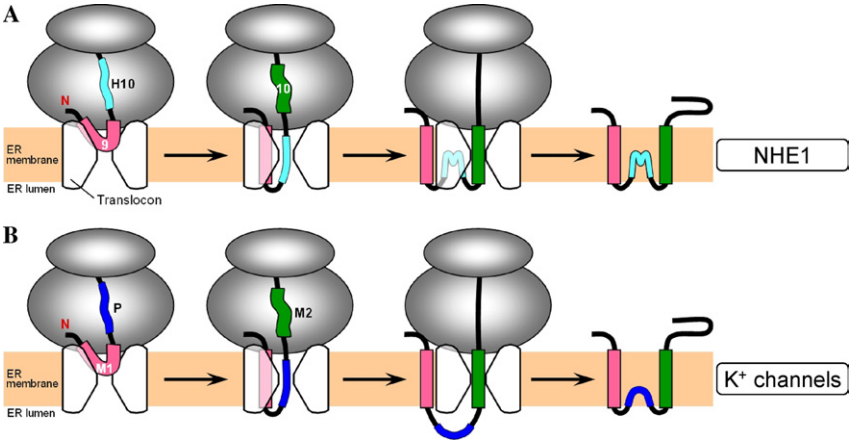

Fig. 4. Two different modes of integration of embedded membrane loop segments. (A) TM9 (magenta) initiates the translocation of the following polypeptide chain. The following H10 (blue) is translocated through but kept in the membrane as an intervening loop, so that the processing and glycosylation sites in front of the H10 segment are not accessible to the enzymes. TM10 (green) interrupts the translocation and becomes the TM segment. (B) The pore loop (P) of the K^+-channel between two transmembrane segments (M1 and M2) is once exposed in the ER lumen before the channel achieves the final membrane topology, even though they are embedded in the membrane in the final structure.

Next, we addressed the possibility of signal peptidase processing. According to the prediction by SignalP-NN [22], there were two candidate processing sites of A^{369}–N^{370} and G^{405}–S^{406} (Fig. 3B). The former potential site in the T^{377}-construct was destroyed by point mutation from A^{369} of the processing site to Pro or Phe (Fig. 3A). Both Pro and Phe should be unfavorable signal processing [23]; the prediction of the mutated sequence also had a low processing score (Fig. 3B). When the mutants were synthesized in the presence of RM and treated with the EndoH, the lower molecular weight bands were remarkably decremented in comparison to the original T^{377}-construct, as expected (Fig. 3A, compare arrowheads in lanes 3, 11, and 15). In the case of the H^{408}-construct, a processed band with similar molecular weight to that of the T^{377}-construct was also observed (Fig. 2A, an arrowhead in lane 19). It is highly likely that the second potential processing site (G^{405}–S^{406}) was processed in this case. The results indicated that the heterogeneity was due to the partial modifications of the glycosylation and processing sites within the constructs. The modifications do not occur when the full H10 segment is present in the constructs.

To exploit the insulation of H10 from glycosylation enzymes in the lumen, we created glycosylation sites within the H10 segment using amino acid replacements (Fig. 3C). The PL domain used here does not have a glycosylation site. None of the created glycosylation sites were glycosylated (lanes 2, 4, 6, 8, and 10). This result indicates that the H10 segment was not exposed on the ER lumenal side during biosynthesis.

Discussion

The findings demonstrate that the H10 segment of NHE1 is translocated through the ER membrane, positioned in the lumen as a membrane loop between TM9 and TM10, but never exposed in the lumenal space. The direct insertion of the H10 segment into the membrane accompanies sequestration of the preceding segment from the lumenal space (Fig. 4A).

The impressive finding of this work is that there are potential glycosylation and signal peptidase processing sites after TM9, which become accessible to the enzymes only when the lumen reporter domain is fused at the former positions of the H10 segment (Figs. 2 and 3). The active sites of the signal peptidase and oligosaccharyltransferase are more than 10 residues away from the membrane surface [24,25]. The modification sites should never reach these active sites and are directly sequestrated in the membrane domain during topogenesis, as indicated in the model (Fig. 4A). This conclusion shows a clear contrast to the topogenic process of other lumenal loops of channels and transporters; e.g., P-loops of K^+ channels, such as Kir 2.1, KcsA, KAT1, water channel, and the R10 segment of band 3 molecule [10,26]. When artificial glycosylation sites were introduced at various points within the loops, they were modified by the glycosylation enzyme. Incorporation of such loops into the membrane depends on interactions between polypeptide segments and the overall folding of the molecule [10,13]. In these cases, the loop segments are exposed in the lumenal space until the other segments assume the correct confirmation (Fig. 4B). After complete translation, the pore loops are incorporated into the membrane domain [13]. In contrast, it is likely that H10 can be integrated properly without TM10 and that H10 possesses the capacity to form the membrane loop structure alone, although it does not interrupt translocation.

Akiyama et al. [27] demonstrated that there is a cryptic processing site for leader peptidase just after the TM5 segment of the SecY molecule. In this case, the processing site is sequestrated from the enzyme by the following TM segment. The findings of the H10 segment suggest that the lumenal loop can also mediate sequestration of potential processing sites and N-glycosylation sites from the modification enzymes.

In Na^+/H^+ exchanger isoform 1 of *A. thaliana* (AtNHX1), TM9 of AtNHX1, which is an orthologous region of H10 segment of human NHE1, was reported to be a complete TM with N_{exo}/C_{cyt} orientation. The C-terminal side from TM10 in AtNHX1 is assumed to be the inverse to that of human NHE1 [28]. Further studies are required to examine whether or not such different results are due to the topological heterogeneity within the NHE/NHX gene family.

Acknowledgments

This work was supported by Grants-in-Aid for scientific research from the Ministry of Education, Science, Sports and Culture of Japan (to K.M. and M.S.), and by Takeda Science Foundation (to K.M.). Y.S. is supported by grants from the Research Fellowships of the Japan Society for the Promotion of Science for Young Scientists.

References

[1] M. Sakaguchi, Eukaryotic protein secretion, Curr. Oppin. Biotech. 8 (1997) 595–601.
[2] P. Walter, A.E. Johnson, Signal sequence recognition and protein targeting to the endoplasmic reticulum membrane, Annu. Rev. Cell Biol. 10 (1994) 87–119.
[3] A.E. Johnson, M.A. van Waes, The translocon: a dynamic gateway at the ER membrane, Annu. Rev. Cell Dev. Biol. 15 (1999) 799–842.
[4] Y. Kida, M. Sakaguchi, M. Fukuda, K. Mikoshiba, K. Mihara, Membrane topogenesis of a type I signal-anchor protein, mouse synaptotagmin II, on the endoplasmic reticulum, J. Cell Biol. 150 (2000) 719–729.

[5] M. Sakaguchi, N. Hachiya, K. Mihara, T. Omura, Mitochondrial porin can be translocated across both endoplasmic reticulum and mitochondrial membranes, J. Biochem. 112 (1992) 243–248.
[6] S. High, B. Dobberstein, Mechanisms that determine the transmembrane disposition of proteins, Curr. Opin. Cell Biol. 4 (1992) 581–586.
[7] M. Sakaguchi, Autonomous and heteronomous positioning of transmembrane segments in multispanning membrane protein, Biochem. Biophys. Res. Commun. 296 (2002) 1–4.
[8] K. Ota, M. Sakaguchi, G. von Heijne, N. Hamasaki, K. Mihara, Forced transmembrane orientation of hydrophilic polypeptide segments in multispanning membrane proteins, Mol. Cell 2 (1998) 495–503.
[9] K. Ota, M. Sakaguchi, N. Hamasaki, K. Mihara, Assessment of topogenic functions of anticipated transmembrane segments of human band 3, J. Biol. Chem. 273 (1998) 28286–28291.
[10] T. Kanki, M. Sakaguchi, A. Kitamura, T. Sato, K. Mihara, N. Hamasaki, The tenth membrane region of band 3 is initially exposed to the luminal side of the endoplasmic reticulum and then integrated into a partially folded band 3 intermediate, Biochemistry 41 (2002) 13973–13981.
[11] Y. Sato, M. Sakaguchi, S. Goshima, T. Nakamura, N. Uozumi, Molecular dissection of the contribution of negatively and positively charged residues in S2, S3, and S4 to the final membrane topology of the voltage sensor in the K^+ channel, KAT1, J. Biol. Chem. 278 (2003) 13227–13234.
[12] Y. Sato, M. Sakaguchi, S. Goshima, T. Nakamura, N. Uozumi, Integration of Shaker-type K^+ channel, KAT1 into the endoplasmic reticulum membrane: synergistic insertion of voltage sensing segments, S3–S4 and independent insertion of pore-forming segments, S5–S6, Proc. Natl. Acad. Sci. USA 99 (2002) 60–65.
[13] N. Umigai, Y. Sato, A. Mizutani, T. Utsumi, M. Sakaguchi, N. Uozumi, Topogenesis of two transmembrane type K^+ channels, Kir 2.1 and KcsA, J. Biol. Chem. 278 (2003) 40373–40384.
[14] S. Wakabayashi, T. Pang, X. Su, M. Shigekawa, A novel topology model of the human Na^+/H^+ exchanger isoform 1, J. Biol. Chem. 275 (2000) 7942–7949.
[15] S. Wakabayashi, M. Shigekawa, J. Pouysségur, Molecular physiology of vertebrate Na^+/H^+ exchangers, Physiol. Rev. 77 (1997) 51–74.
[16] P. Walter, G. Blobel, Preparation of microsomal membranes for co-translational protein translocation, Methods Enzymol. 96 (1983) 84–93.
[17] R.J. Jackson, T. Hunt, Preparation and use of nuclease-treated rabbit reticulocyte lysates for the translation of eukaryotic messenger RNA, Methods Enzymol. 96 (1983) 50–74.
[18] R.M. Horton, S.N. Ho, J.K. Pullen, H.D. Hunt, Z. Cai, L.R. Pease, Gene splicing by overlap extension, Methods Enzymol. 217 (1993) 270–279.
[19] K. Ota, M. Sakaguchi, N. Hamasaki, K. Mihara, Membrane integration of the second transmembrane segment of band 3 requires a closely apposed preceding signal-anchor sequence, J. Biol. Chem. 275 (2000) 29743–29748.
[20] M. Popov, L.Y. Tam, J. Li, R.A.F. Reithmeier, Mapping the ends of transmembrane segments in a polytopic membrane protein, J. Biol. Chem. 272 (1997) 18325–18332.
[21] Y. Kato, M. Sakaguchi, Y. Mori, K. Saito, T. Nakamura, E.P. Bakker, Y. Sato, S. Goshima, N. Uozumi, Evidence in support of a four transmembrane-pore-transmembrane topology model for the *Arabidopsis thaliana* Na^+/K^+ translocating AtHKT1 protein, a member of the superfamily of K^+ transporters, Proc. Natl. Acad. Sci. USA 98 (2001) 6488–6493.
[22] H. Nielsen, J. Engelbrecht, S. Brunak, G. vonHeijne, Identification of prokaryotic and eukaryotic signal peptides and prediction of their cleavage sites, Protein Eng. 10 (1997) 1–6.
[23] G. von Heijne, The signal peptide, J. Membr. Biol. 115 (1990) 195–201.
[24] P. Whitley, I.M. Nilsson, G. von Heijne, A nascent secretory protein may traverse the ribosome/endoplasmic reticulum translocase complex as an extended chain, J. Biol. Chem. 271 (1996) 6241–6244.
[25] I.M. Nilsson, G. von Heijne, Determination of the distance between the oligosaccharyltransferase active site and the endoplasmic reticulum membrane, J. Biol. Chem. 268 (1993) 5798–5801.
[26] T. Kanki, M.T. Young, M. Sakaguchi, N. Hamasaki, M.J. Tanner, The N-terminal region of the transmembrane domain of human erythrocyte band 3. Residues critical for membrane insertion and transport activity, J. Biol. Chem. 278 (2003) 5564–5573.
[27] Y. Akiyama, T. Inada, Y. Nakamura, K. Ito, SecY, a multispanning integral membrane protein, contains a potential leader peptidase cleavage site, J. Bacteriol. 172 (1990) 2888–2893.
[28] T. Yamaguchi, M.P. Apse, H. Shi, E. Blumwald, Topological analysis of a plant vacuolar Na^+/H^+ antiporter reveals a luminal C terminus that regulates antiporter cation selectivity, Proc. Natl. Acad. Sci. USA 100 (2003) 12510–12515.
[29] J. Kyte, R.F. Doolittle, A simple method for displaying the hydropathic character of a protein, J. Mol. Biol. 157 (1982) 105–132.